

1 **Preliminary hand-held thermal imaging results of sequential**  
2 **monitoring of a simulated deceased individual on terrestrial**  
3 **ground**

4 Kristopher D. Wisniewski Ph.D.<sup>1,2\*</sup>, Jamie K. Pringle Ph.D.<sup>2</sup>, Vivienne Heaton Ph.D.<sup>3</sup> &  
5 Andrew J. Mitten M.Geol<sup>1</sup>

6 <sup>1</sup>Department of Criminal Justice and Forensics, School of Law, Policing & Forensics,  
7 Science Centre, Staffordshire University, Leek Road, Stoke on Trent, ST4 2DF, UK.

8 <sup>2</sup>School of Geography, Geology and Environment, Keele University, Keele, Staffs, ST5 5BG,  
9 UK.

10 <sup>3</sup>School of Chemical and Physical Sciences, Keele University, Keele, Staffs, ST5 5BG, UK.

11 Emails: [kristopher.wisniewski@staffs.ac.uk](mailto:kristopher.wisniewski@staffs.ac.uk) ; [j.k.pringle@keele.ac.uk](mailto:j.k.pringle@keele.ac.uk); [v.g.heaton@keele.ac.uk](mailto:v.g.heaton@keele.ac.uk) ;  
12 [a.j.mitten@keele.ac.uk](mailto:a.j.mitten@keele.ac.uk)

13 \*Corresponding author: K. D. Wisniewski ([kristopher.wisniewski@staffs.ac.uk](mailto:kristopher.wisniewski@staffs.ac.uk))

14

15 **ABSTRACT**

16

17 Thermal imaging is commonly used by forensic search investigators to locate  
18 missing persons, and can be used to detect thermal targets in darkness, but there is  
19 little research on its actual effectiveness to detect individuals after death. This paper  
20 aims to determine how long hand-held thermal imaging is effective to detect a naked  
21 body lying on the surface for and when is the optimal time to survey.

22 A simulated murder victim, using a freshly dispatched pig (*Sus scrofa*) carcass, was  
23 left on the soil surface of a test site and imaged three times a day until active body  
24 decomposition was complete (TBS of 35) which was 61 days. Images were  
25 quantitatively analysed to determine what the relative thermal response the cadaver  
26 had with respect to background site values, with results corrected for daily  
27 temperature variations (ADD) and decomposition stages (TBS scores).

28 Results evidenced the surface cadaver was detectable throughout active  
29 decomposition, but optimal survey time depended on decomposition stage. Morning  
30 surveys were found to be optimal up to 10 days PMI (0-90 ADD, 0-4 TBS),  
31 evening/dusk surveys optimal from 10 to 40 days PMI (90-400 ADD, 4-26 TBS),  
32 midday surveys optimal from 40 to 50 days PMI (400-530 ADD, 26-29 TBS) and then  
33 evening surveys to the end of the 61-day (530-680 ADD, 29-35 TBS) study period.

34 Implications suggest that thermal imaging is recommended to detect missing  
35 persons even after death and surveys should be undertaken at specific time periods  
36 during the day to improve search detection success if PMI can be estimated.

37

38 **KEYWORDS: forensic science, thermal, search, surface remains, survey,**  
39 **missing persons**

40

41 **Highlights**

- 42 • Study to quantify effectiveness of thermal imaging surveys for missing persons
- 43 • Decomposing cadaver thermally detected up to 61 days PMI (681 ADD, 35 TBS)
- 44 • Thermal anomaly low/high relative to background depending on survey
- 45 • When survey undertaken during the day also important
- 46 • Surveying needs to account for decomposition stage to optimise results

47

48 **Role of the funding source**

49 This research did not receive any specific grant from funding agencies in the public,  
50 commercial, or not-for-profit sectors.

51 **Acknowledgements**

52 The Nuffield Foundation are thanked for providing financial support for summer  
53 Further Education studentships. Keele University estates team are thanked for  
54 allowing site access and logistical support. Liz Deakin of Staffordshire University is  
55 thanked for logistical support. This project was undertaken on a DEFRA-approved  
56 controlled test area and gained School ethical approval.

57

58 **Introduction**

59

60 The use of forensic geoscientific techniques and methods in the search for missing  
61 persons is increasing; as locating them is of vital importance for their families and for  
62 criminal convictions to proceed (1). Current forensic search methods are highly  
63 varied and have been reviewed elsewhere (1,2), with best practice suggesting a  
64 phased approach, moving from large-scale remote sensing techniques (3) to ground  
65 reconnaissance and control studies before full searches are initiated (4). Full  
66 searches have involved a variety of methods, including forensic geomorphology (5),  
67 forensic botany (6,7), entomology (8) and scent-trained search dogs (9,10).

68 Remote sensing has commonly been used at both the large scale, where potential  
69 positions are identified, (see 2,11) and at smaller scales, such as using infrared  
70 imaging to capture blood spatter patterns at crime scenes (12), or diagnosing death  
71 by fire (13). Hyperspectral imagery is a common technique for detecting both  
72 explosive residues (14), trace evidence (e.g. 15) and even providing age estimations  
73 of blood stains (see 16). Originally adopted for military use in the 1950s, thermal  
74 detection has been utilised for the detection of landmines (17) and Improvised  
75 Explosive Devices (IEDs) (18). In forensics thermal imaging is commonly used to  
76 detect fleeing fugitives and heat by-products of illegal cannabis operations (19), and  
77 even facial analysis to detect intoxication (20).

78 Recent forensic research has used control studies to determine optimal body  
79 detection method(s) and equipment configuration(s). Results can be highly variable,  
80 depending upon a large number of factors, the most important being postmortem  
81 interval (PMI), body wrapping, local soil type, vegetation and climate (21-30).  
82 However, there has been little controlled research into the effectiveness of thermal  
83 imaging to detect surface remains after death.

84 Depending on climatic conditions, a body will cool after death, reaching ambient  
85 temperatures within ~24 h (31), thus providing no detectable thermal contrast.  
86 However, the human body has a higher specific heat capacity (~3,500 J/Kg °C) (32),  
87 when compared to typical wet (~1480 J/Kg °C) and dry (~800 J/Kg °C) soil (33).  
88 Therefore, even when deceased, it will take longer for a human body to warm up and  
89 cool down, particularly at dawn and dusk when temperature changes are at their  
90 most rapid. Bone has a much lower specific heat capacity (~440 J/Kg °C) and thus  
91 should also be able to be differentiated from background soil, with the contrast  
92 greatest in wet soil. It is also commonplace for necrophagous insects, particularly  
93 blowflies, to colonise a corpse immediately following death, given appropriate  
94 environmental conditions (34-37). Female flies will oviposit eggs on the cadaver,  
95 targeting natural orifices, wound sites and folds in clothing (38,39). These eggs will  
96 hatch after ~6 h - 40 h, depending on species and ambient temperature, and first  
97 instar larvae will immediately begin feeding on soft tissue (34). During this feeding  
98 phase larvae will aggregate, usually during second and third larval instar (34,35), to  
99 form a 'maggot mass'. Masses, often composed of thousands of larvae, generate  
100 significant levels of heat as a result of feeding and fast metabolisms, particularly  
101 during active body decay. Controlled laboratory research has shown masses  
102 containing as few as 1,200 larvae producing significantly warmer than ambient

103 temperatures (40), whilst field studies using animal proxies have recorded mass  
104 temperatures up to 50°C (36,41,42). Not only does mass size mass influence heat,  
105 but also density (43), species composition (44), stage of larval development (45),  
106 and sun exposure (46).

107 This paper's aims are to investigate: (1) the length of time that a surface cadaver  
108 would be detectable for during active decomposition, using hand-held thermal  
109 imaging and (2) the optimal time of day for undertaking such a thermal imaging  
110 survey.

111

Pre-print

## 112 **Materials and methods**

### 113 **Study test site**

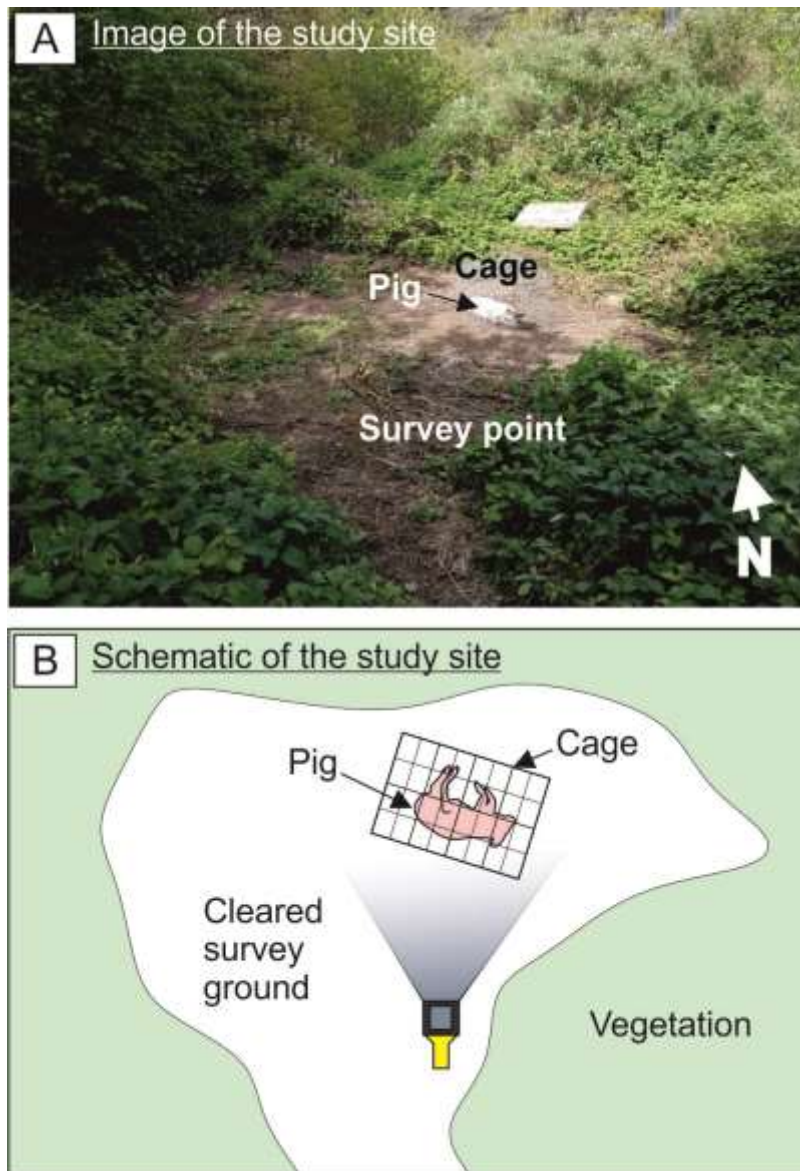
114 The test site at Keele University, Staffordshire, is situated in a restricted area of  
115 grassed semi-rural ground surrounded by deciduous woodland and hedges (FIG. 1).  
116 The site lies ~200 m above sea level. The local soil is a sandy loam with nearby  
117 borehole records (27) with a bedrock of Carboniferous (Westphalian) Butterton  
118 Sandstone bedrock present at ~2.5 m below ground level (bgl). This site has been  
119 previously used for forensic geophysical studies (27-29,47) but these are downslope  
120 of this investigation site so avoiding any soil contamination issues.

121 Surveying was carried out between the 10th April and 9th June 2017, when warmer  
122 temperatures would facilitate insect cadaver activity, and surveying continued until  
123 active decomposition was complete, i.e. when the Total Body Score (following (54)  
124 method) reached 35. Meteorological data was available from the weather station  
125 situated ~200 m east of the study site. Average monthly rainfall was 24 mm  
126 (April/May) and 70.2 mm (June), with average daily air temperatures varied from 6.6  
127 °C to 23.6 °C and averaged 13.7 °C over the study period. Having temperature data  
128 allowed Accumulated Degree Days (ADD) to be calculated which corrects for local  
129 site temperature variations (see (21) for details).

### 130 **Pig cadaver**

131 The use of pig cadavers as human analogues is well established in forensic science  
132 studies as they have similar chemical compositions, body sizes, tissue-to-body fat  
133 ratios, gut fauna, skin/hair types, and emissivity value to humans (27,28,48-50). At  
134 the current research site their use has been approved by the Department for  
135 Environment, Food & Rural Affairs (DEFRA) and the School's Ethics Committees.

136 A single, naked, (~31 kg) pig (*Sus scrofa*) cadaver, sourced from a local abattoir and  
137 dispatched by a bolt gun to the temporal bone less than 6 h beforehand, was placed  
138 on the ground surface that was cleared of any vegetation (FIG. 1). Within 30 minutes  
139 of exposure adult blow flies identified as *Lucilia sericata* and *Calliphora vicina* were  
140 observed ovipositing eggs on the head, specifically in the eyes, ears, nose and  
141 mouth. Later that day the same species were observed in the region of the genitals.  
142 These two blow fly species are typical for the region and frequently observed at the  
143 research site from March through to September/October. During days 2-3, the eggs  
144 eclosed and first instar larvae emerged, aggregating to form two masses, one on the  
145 head and another in the genitals, each consisting of several thousand individuals.  
146 Exact larval numbers could not be determined, since the majority of mass fed  
147 internally, commencing at the head and genitals before progressing into the  
148 abdomen. The pig cadaver had a metal cage placed over the top after each survey  
149 to avoid/reduce scavenging activities.



150

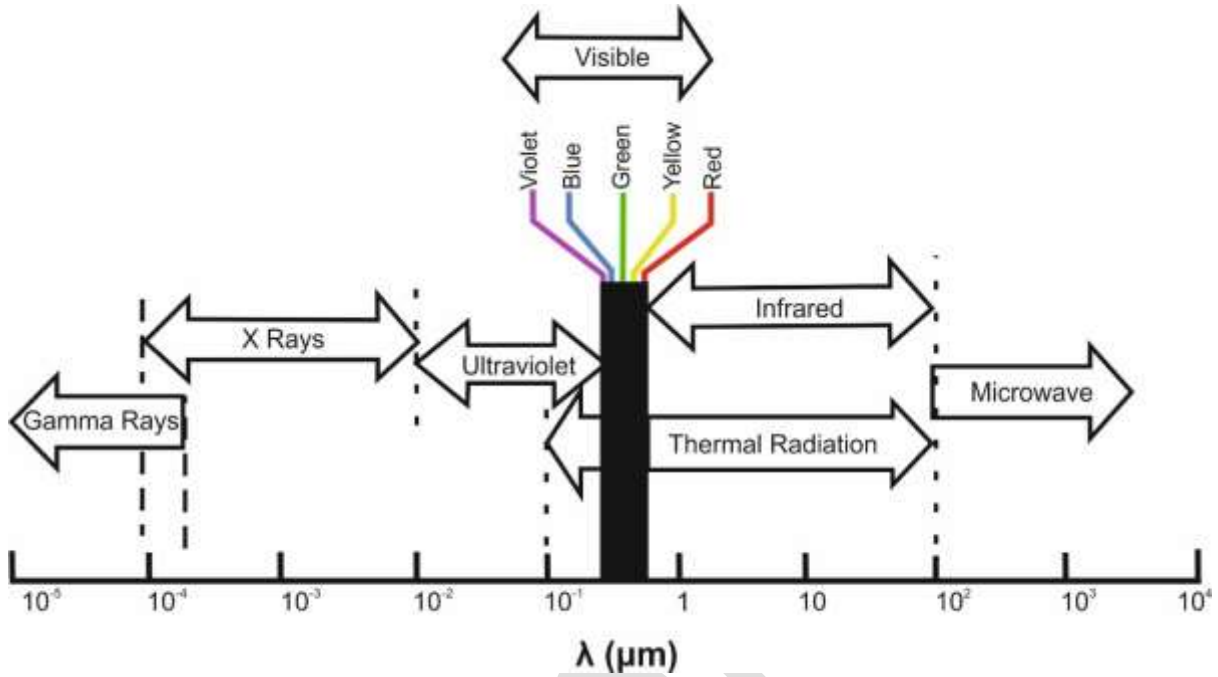
151 **FIG. 1.** A) Image and B) schematic of survey site, survey point denotes location  
 152 where all thermal image data were acquired (2.5 m from cadaver).

153

154 **Thermal radiation**

155 At temperatures above absolute zero all objects emit radiation (12) which can loosely  
 156 be considered as 'thermal radiation' (51). At terrestrial temperatures thermal  
 157 radiation, consisting primarily of self-emitted and secondarily of reflected radiation

158 from other heat sources, is emitted predominately at a wavelength band of 3 μm - 14  
 159 μm of the electromagnetic spectrum (51) (see FIG. 2).



160

161 **FIG. 2.** Electromagnetic radiation spectrum (after, (52)).

162

163 Although hypothetical in thermal radiation theory, a *blackbody* is an object that  
 164 absorbs all radiant energy, thus appearing black at all wavelengths. A blackbody will  
 165 also emit a continuous spectrum of wavelengths (53). Stefan–Boltzman’s law (Eq. 1)  
 166 describes the relationship between the total emission of radiant energy of a  
 167 blackbody and its absolute temperature.

168 
$$P_t = \sigma T^4 \quad (1)$$

169 Where  $P_t$  = total power emitted by a blackbody ( $\text{W}/\text{m}^2$ ),  $\sigma$  = Stefan–Boltzmann  
 170 constant ( $5.67 \times 10^{-8} \text{ W}/\text{m}^2 \text{ K}^4$ ), and  $T$  = absolute temperature in K. However, since  
 171 blackbodies do not exist in nature, Stefan Boltzman’s law is modified to give (Eq. 2):

172

$$P_t = \varepsilon\sigma T^4 \quad (2)$$

173 Here,  $\varepsilon$  = emittance of the surface ( $\varepsilon = 1$  for a blackbody). The emissivity of a surface  
174 is defined as the ratio of the energy absorbed by the surface to the energy absorbed  
175 by a blackbody. Consequently, all surfaces will have an emissivity value between 0  
176 and 1 (53). During day time surveys all measured radiation will include reflected  
177 radiation, with the major component being solar radiation (53). Other sources of  
178 radiation will also be detected i.e. if the target is self-heating (51). Most mammal  
179 skins have emissivities greater than 0.9, making them a good emitter/radiator, but a  
180 poor reflector of thermal radiation. Both human (54) and pig skin (50) have an  
181 emissivity of 0.98. In contrast, a shiny surface (e.g.  $\varepsilon = < 0.2$ ) is a poor absorber and  
182 a poor emitter but a good reflector of thermal radiation (53).

183 A warmer/cooler object ( $P_o$ ) will continue to emit/absorb thermal radiation until it  
184 reaches equilibrium with its surroundings ( $P_b$ ). Thermal imagers are able to  
185 distinguish between objects of the same temperature due to their contrasting  
186 emissivities. A thermal imager is only able to detect the differences between emitted  
187 powers (Eq. 1) and not absolute temperatures:

188

$$\Delta P = P_o - P_b \quad (1)$$

189 The benefits of thermal imaging, compared to photographs, is that it does not rely on  
190 visible light, but instead thermal energy, making it possible to detect targets in total  
191 darkness, through low visibility (e.g. smoke and fog) and in low contrast situations.

## 192 **Thermal imaging surveys**

193 A Fluke™ TiR125 thermal imaging camera was used for this study that acquires  
194 quantitative temperature matrix data (\*.IS2 format) over the surveyed area - this

195 camera has an accuracy of 0.1 °C. This allows quantitative comparisons of repeat  
196 thermal image data to be calculated. A thermal emissivity correction of 0.98 was  
197 used for all the thermal images as 0.98 is emissivity of both pig/human skin (see 50,  
198 54). After initial equipment testing, the instrument was used following the equipment  
199 manufacturers instructions, in particular, for the instrument to warm up for ~15 mins  
200 before each thermal imaging survey was undertaken to optimise results.

201

202 Immediately after the pig cadaver had been placed on the cleared ground surface on  
203 day 1, an initial thermal imaging survey was undertaken, with readings taken at 2 h -  
204 3 h intervals over a 24 h period, in order to determine when optimal survey time(s)  
205 for the subsequent thermal imaging surveys should be undertaken. During the first  
206 24 hours the thermal anomaly over the pig cadaver changed diurnally, from a relative  
207 high anomaly, with respect to background values, during midday and evening  
208 surveys to no thermal anomaly overnight and a relative low anomaly in the morning  
209 (see FIG. 3). Therefore, the best times for the subsequent thermal surveys over this  
210 pig cadaver were noted to be ~08:00-09:59 (morning), ~12:00-13:59 (Midday) and  
211 ~20:00 to 21:59 (evening) respectively, due to there being a good thermal response  
212 over the surface pig cadaver, when compared to background site values (FIG. 3).

213

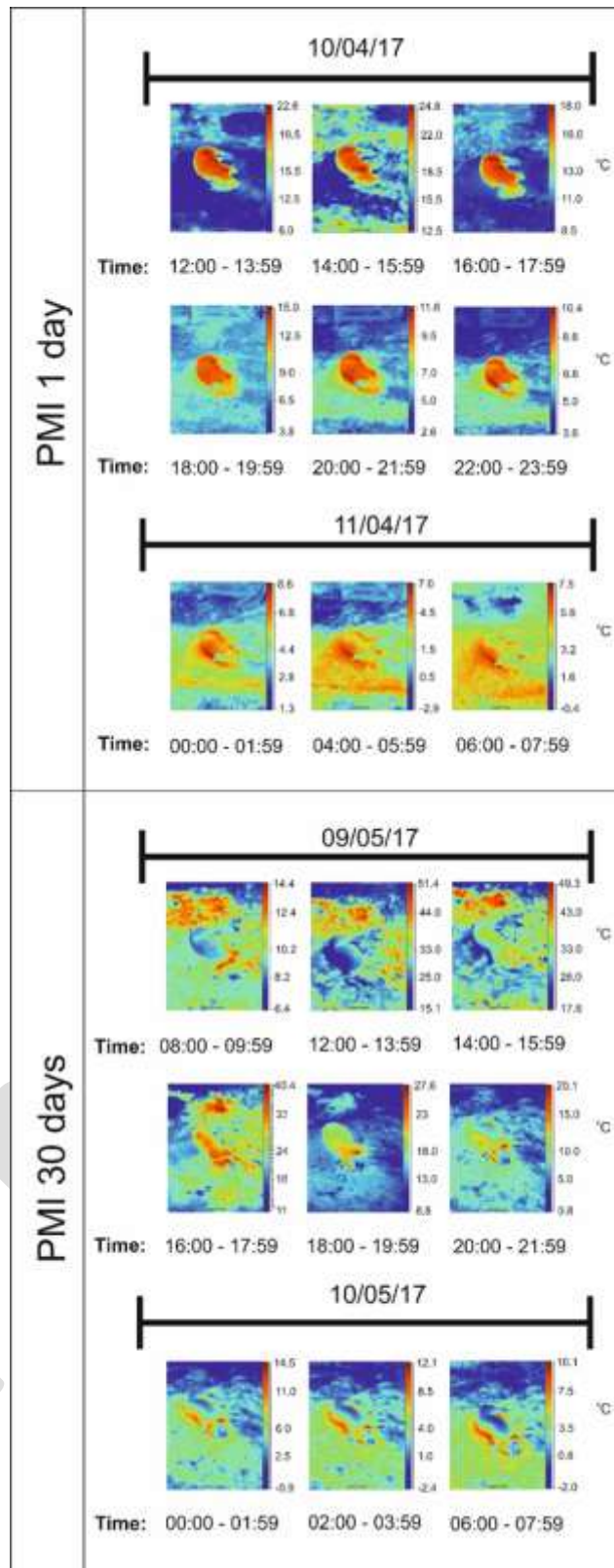
214 The subsequent daily thermal imaging surveys over the surface pig cadaver,  
215 throughout the course of the survey period, were then taken at these three chosen  
216 time periods up to day 49; after this, daily surveys were only taken up to day 61 at  
217 evening survey times due to equipment availability. By day 61 the Total Body Score  
218 (TBS) of 35 was reached, which signifies the end of the active decomposition period

|  
219 (see 55) and thus this experiment. Vegetation regrowth had also meant thermal  
220 surveys were taking vegetation temperature by this point. Throughout the thermal  
221 survey experiment, each thermal image was taken from the same marked location  
222 (see FIG. 1) by the same operator at a set height of 1.4 m above the ground for  
223 consistency purposes.

224

225

Pre-print



226

227 FIG. 3 -Graphical summary of day 1 and day 30 thermal image surveys collected  
 228 over the surface pig cadaver every 2-3 h, each over a 24 h survey period (times  
 229 given).

230

231 **Thermal image data analysis**

232

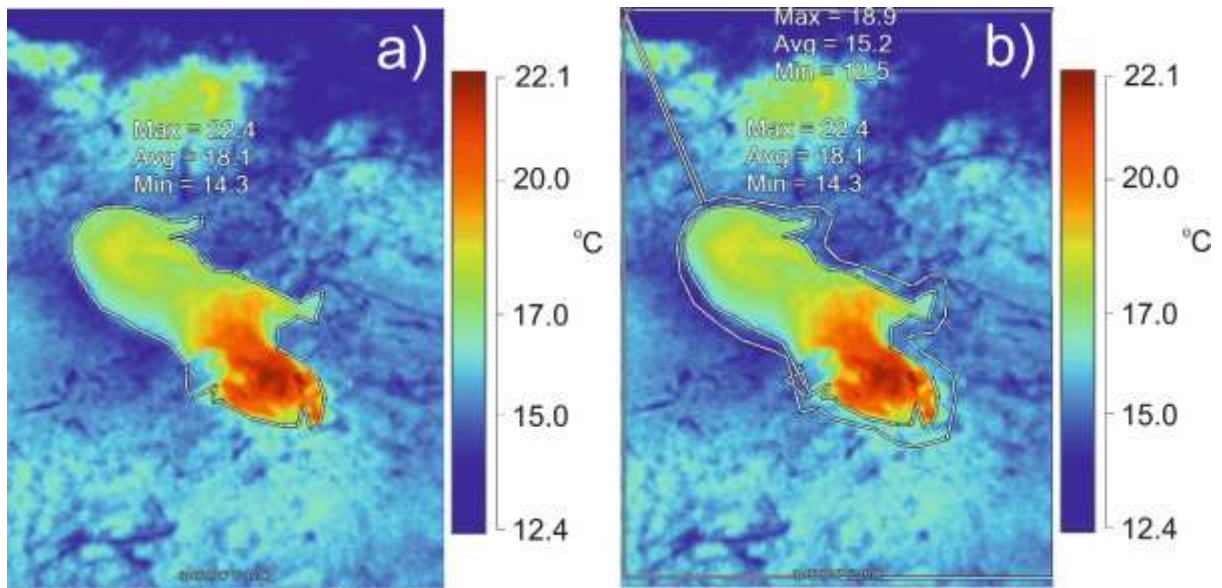
233 Fluke SmartView® 4.3 software was used for thermal temperature matrix image data  
234 processing. . Digital polygons were manually added on each digital thermal image  
235 matrix, which allowed the differentiation between the respective pig cadaver and  
236 background area, to obtain minimum/average/maximum thermal image temperatures  
237 (see FIG. 4 for example). The thermal difference data, between pig and background,  
238 from the study was treated separately, dependent upon the time of day it was  
239 collected. This data was then plotted against postmortem interval (PMI) and  
240 accumulated degree days (ADD; the latter correcting for daily temperature  
241 fluctuations). A simple 5-point moving average was then fitted to the thermal  
242 difference data so that single anomalous weather variations were minimised.

243 Total Body Scores (TBS) were also assigned during regular site visits; with TBS  
244 being the current standard forensic anthropology method used to quantify active  
245 decomposition (see 55). The PMI, ADD and TBS data were then summarised, and  
246 the type (positive or negative) of relative thermal anomaly, when compared to  
247 background values, that a surface cadaver would produce.

248

249

250



251

252 **FIG. 4.** Graphical summary detailing an example of thermal image data processing  
 253 used in this study. A digital polygon was drawn around a) the surface pig cadaver  
 254 and b) the background area, with minimum/average/maximum temperature values of  
 255 both a/b areas (shown) extracted.

256

## 257 **Results**

258

259 The thermal signature associated with the pig cadaver, when compared to  
260 background thermal image values, varied as either a low, high or, in fact, no anomaly  
261 being imaged, when compared to background values. This variation was witnessed  
262 across each of the morning, midday and evening surveys (see FIG. 5 and FIG. 6 for  
263 respective thermal image data examples and graphical thermal summaries  
264 throughout the survey period).

265 For PMI days 1-10 (0 ADD - 90 ADD), morning and midday surveys generally had -1  
266 °C to -2 °C anomalies, and evening surveys had +1 °C to +2 °C anomalies over the  
267 surface pig cadaver, when compared to background values respectively. Morning  
268 surveys determined to be optimal over this survey period.

269 For PMI days 10-20 (90 ADD - 170 ADD), morning surveys generally had -1 °C to 0  
270 °C anomalies, midday surveys had -1 °C to +1 °C anomalies, and evening surveys  
271 had +1 °C to +2 °C anomalies over the surface pig cadaver, when compared to  
272 background values respectively. Evening surveys were determined to be optimal  
273 over this survey period.

274 For PMI days 20-30 (170 ADD - 270 ADD), morning surveys generally had -1 °C to 0  
275 °C anomalies, midday surveys had 0 °C to +1 °C anomalies, and evening surveys had  
276 +2 °C to +5 °C anomalies over the surface pig cadaver, when compared to  
277 background values respectively. Evening surveys were determined to be optimal  
278 over this survey period.

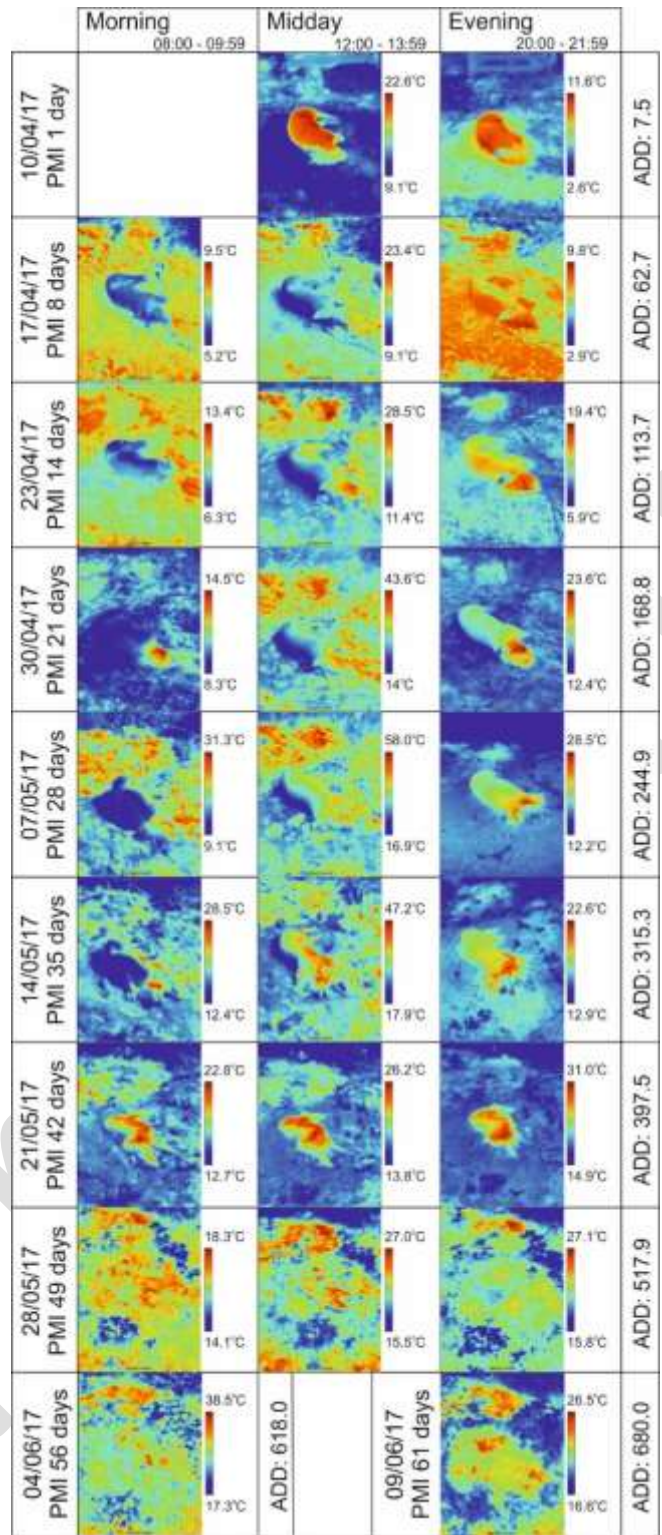
279 For PMI days 30-40 (270 ADD - 400 ADD), morning surveys generally had 0 °C to +2  
280 °C anomalies, midday surveys had +1 °C to +3 °C anomalies, and evening surveys

281 had +2 °C to +4 °C anomalies over the surface pig cadaver, when compared to  
282 background values respectively. Evening surveys were determined to be optimal  
283 over this survey period.

284 For PMI days 40-50 (400 ADD - 530 ADD), morning surveys generally had +2 °C to  
285 +3 °C anomalies, midday surveys had +3 °C to +6 °C anomalies, and evening surveys  
286 had +2 °C to +3 °C anomalies over the surface pig cadaver, when compared to  
287 background values respectively. Midday surveys were determined to be optimal over  
288 this survey period.

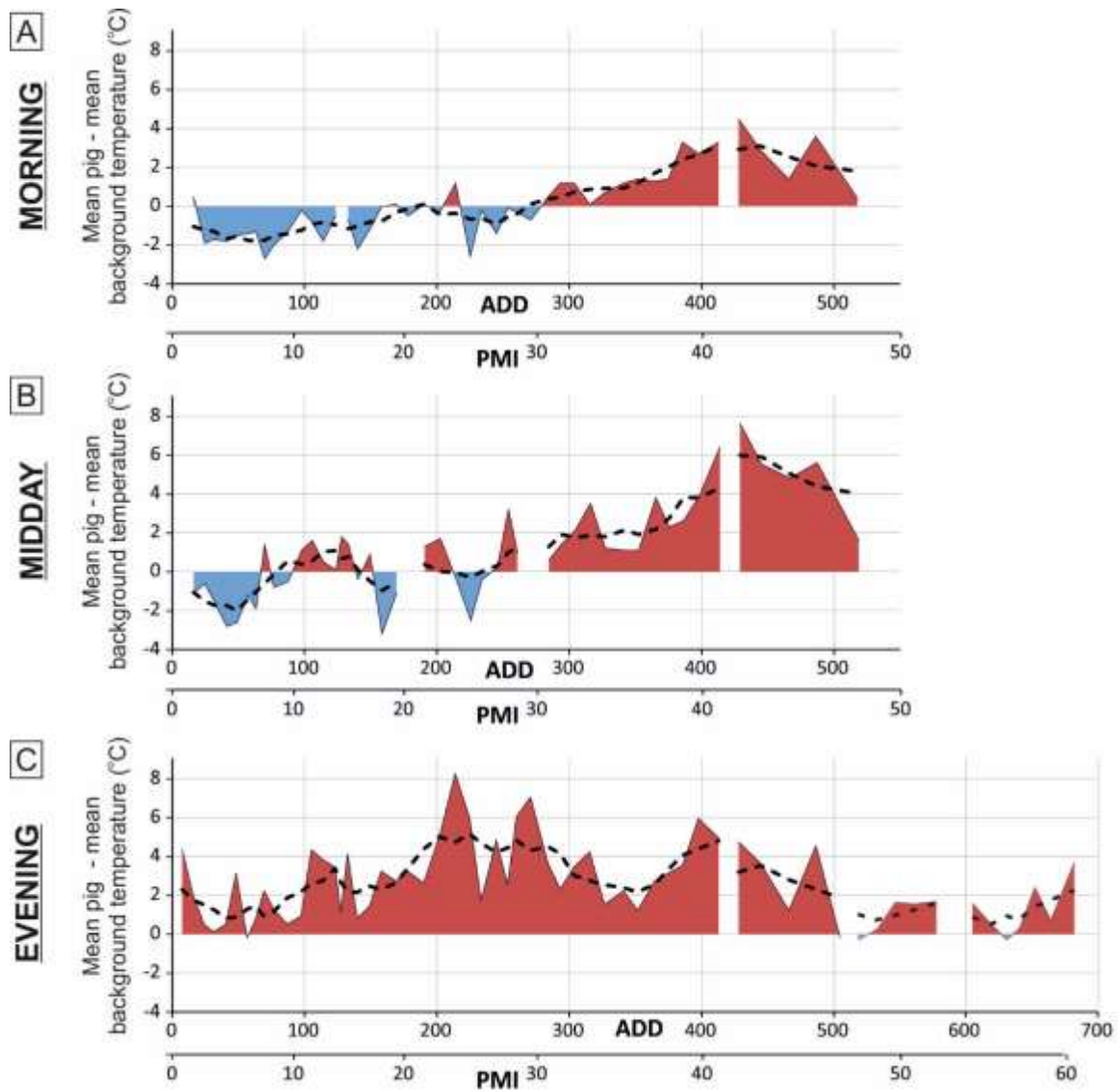
289 For PMI days 50-61 (530 ADD - 680 ADD), evening surveys had +1 °C to +2 °C  
290 anomalies over the surface pig cadaver, when compared to background values  
291 respectively.

292 Table 1 summarises these key findings which, as well as including the PMI, also  
293 includes the Accumulated Degree Days (ADD) and Total Body Scores (TBS) of the  
294 target surface cadaver. Finally, it also summarises the perceived optimal time during  
295 the day for a thermal imaging survey to be undertaken as discussed here.



296

297 FIG. 5- Thermal image survey examples taken over the study period (PMI/ADD  
 298 shown for comparison). Note the morning, midday and evening surveys and thermal  
 299 anomaly over the surface pig cadaver varies as either low, no anomaly or high  
 300 anomaly with respect to background values.



302

303 **FIG. 6.** Graphical summary of thermal imaging data quantitative analysis, showing  
 304 the relative thermal difference (average pig anomaly minus background values) for  
 305 (a) morning, (b) midday and, (c) evening surveys respectively. Dotted line gives five-  
 306 point running average values. Note bottom axes are both Post-Mortem Interval (PMI)  
 307 and Accumulated Degree Days (ADD), see text for details.

308

PMI (days)	ADD (°C)	TBS	Morning anomaly (°C)	Midday anomaly (°C)	Evening anomaly (°C)	Optimal time for thermal survey
0-10	0-90	0-4	-1 to -2	-1 to -2	+1 to +2	Morning
10-20	90-170	5-12	-1 to 0	-1 to +1	+2 to +3	Evening
20-30	170-270	13-20	-1 to 0	0 to +1	+2 to +5	Evening
30-40	270-400	20-26	0 to +2	+1 to +3	+2 to +4	Evening
40-50	400-530	26-29	+2 to +3	+3 to +6	+2 to +3	Midday
50-61	530-680	29-35			+1 to +2	Evening

309

310 **Table 1.** Thermal imaging summary of relative average temperatures of surface pig

311 cadaver minus background values. PMI = Postmortem interval (days), ADD =

312 Accumulated Degree Days, TBS = Total Body Score, see (54) and text for details.

313

314

315 **Discussion**

316

317 This paper's first stated aim was '*the length of time that a surface cadaver would be*  
318 *detectable for during active decomposition*'. From the results of this study, thermal  
319 imaging surveys could detect the surface remains of the pig cadaver during active  
320 decomposition (61 days PMI / 681 ADD / 35 TBS). Two studies, using a ground-  
321 based study (56), similar to this study, and using airborne helicopter thermal imagery  
322 (57), have shown detectable [elevated] thermal signatures of maggot masses on pig  
323 carcasses, but only over more limited 14- and 21-day survey periods, respectively.  
324 This supports the findings reported elsewhere (58), following investigations into  
325 whether thermal imaging could successfully be used to detect thermal emissions on  
326 seven pig cadavers as they decomposed in woodland in New England, USA. Pig  
327 cadavers were detectable between 2- and 26-days PMI, largely due to the larval  
328 aggregations colonising the cadavers, which generated significant amounts of heat.  
329 By day 26 the cadavers had reached the advanced stage of decay, and the absence  
330 of any remaining soft tissues caused the larval masses to disperse away from the  
331 remains and all associated heat to be lost, signifying the end of their experiment  
332 (58). It is possible that the cadaver used in the current research was detectable for  
333 longer due to the cooler ambient temperatures recorded at Keele, slowing the rate of  
334 decomposition and allowing soft tissue to persist for longer, which would support the  
335 larval communities over an extended period of time.

336 The advantage of using the Fluke™ TiR125 thermal imaging camera was that the  
337 data can be saved quantitatively and analysed, particularly to calculate average  
338 temperature differences of the anomaly over the pig cadaver when compared to the  
339 background study site area. This is an important development for such thermal

340 monitoring studies; rather than simply producing an image that could only be  
341 qualitatively assessed, and has other broad forensic applications, not just for thermal  
342 imaging, but perhaps for other search technique data types, for example electrical  
343 resistivity datasets (see (59)).

344 This paper's second stated aim was '*to investigate the optimal time of day for*  
345 *undertaking such a thermal imaging survey*'. Surprisingly this was found to be  
346 important, with different times of day determined to be optimal for surveying, which  
347 seemed to depend upon the PMI and TBS values (Table 1). This should therefore be  
348 of great interest and use to forensic search teams if the PMI/ADD of the missing  
349 individual is known. If the thermal imaging survey is taken at the optimum time, then  
350 search teams should have the greatest chance of success at detecting the missing  
351 individual, which could potentially maximise any remaining forensic evidence,  
352 advance the case efficiently, reduce expenditure and provide more rapid closure for  
353 the victim's family.

354 As decomposition enters the active stage, the relative thermal anomaly over the pig  
355 carcass, with respect to background values became much more elevated. Initially  
356 following death, the remains will cool to ambient, a process known as algor mortis,  
357 making the pig less discernible from its surroundings. However, shortly thereafter  
358 temperatures will increase, likely due to a number of factors including larval  
359 aggregations, bacterial activity and heat loading (40). In regards to heat loading, the  
360 size of the carcass, the nature of the ground it is laid on, and its exposure to direct  
361 sunlight, can all have an effect on its temperature (60). As bodies begin to  
362 decompose the bacteria in the intestines proliferate as they break down the body  
363 further during putrefaction. Some researchers have proposed that bacterial  
364 metabolism plays a significant role in carcass thermogenesis, reporting that even in

365 the absence of maggot masses and solar radiation, cadavers can peak at  
366 temperatures of 32 °C whilst ambient temperature remains a constant 23 °C (56).  
367 Despite these factors, it is the heat generated by feeding larval masses that is  
368 believed to be the biggest contributor to increased localised temperatures recorded  
369 on cadavers. The increase in temperature from ambient correlates with the  
370 emergence of first instar larvae, usually during the bloated stage of decay, and  
371 continues to rise as colonising larvae increase in numbers, as well as in physical  
372 size, with temperatures peaking during the third larval instar and the active stage of  
373 decay (36,40,44,45). It would be during this time, when larval aggregations are at the  
374 hottest, that the use of thermal imagery in searches is most proficient (61). Once  
375 larvae consume the remaining soft tissues on the carcass, they cease feeding and  
376 migrate away from the body in search of a place to pupate and complete  
377 development. It is at this point where temperatures on the cadaver begin to decline,  
378 gradually returning to ambient (40). The thermal anomaly associated with the  
379 remains on day 61 is likely a result of heat absorption by the skeletal elements and  
380 bacterial activity in the soil. The latter was also suggested by a recent study which  
381 reported that carcasses were detectable during the advanced stages of decay using  
382 aircraft mounted thermal imaging due to the soils being contaminated with  
383 decompositional fluids and supporting larger than expected bacterial communities,  
384 resulting in slightly elevated soil temperatures (61). This is likely why all the later  
385 thermal imaging surveys had slightly elevated temperatures regardless of the time of  
386 day that the survey was undertaken.

387 Study limitations included using one and not multiple pig cadavers for replication  
388 purposes and of course this was undertaken on one study site, with unique soil  
389 compositions and local vegetation type. Surveying a wider area on this site may

390 have shown the surrounding vegetation to be poisoned by the release of  
391 decomposition fluids from the cadaver during composition (62), killing the  
392 surrounding vegetation arounds the body and stressing vegetation further away, that  
393 may also be giving a heat signature; this is commonly used in satellite imagery  
394 analysis (63).

395 Since the current research has demonstrated that thermal imaging has the potential  
396 to be used as a search tool for missing persons who are presumed dead, further  
397 investigation should be carried out in order to test its capabilities in a range of  
398 scenarios that may be encountered in casework. This might involve researching its  
399 success at locating bodies wrapped in some form of covering, or drowned victims  
400 floating on the water surface (as below surface victims will not be detectable as  
401 water absorbs IR). Cadavers decomposing in both of these scenarios will be  
402 exposed to insect activity, however insect numbers are expected to be smaller and  
403 more localised as the water and coverings limit larval access. Some researchers  
404 have already investigated the use of aircraft mounted thermal imaging on locating  
405 decomposing remains (57,62), but with current policing budget cuts it may be  
406 worthwhile to look at drone-mounted thermal imaging as a cheaper alternative for  
407 police forces, focusing on their ability to detect remains at different heights, speeds  
408 and over different types of terrain.

409

410 **Conclusion**

411

412 This study aimed to answer fundamental questions on how effective thermal imaging  
413 surveys are to detect deceased individuals on the ground surface using a simulated  
414 individual of a pig (*Sus scrofa*) carcass. Thermal imaging could detect the carcass  
415 over the active decomposition period (61 day, 680 ADD, 35 TBS), with morning  
416 surfaces determined to be optimal from 0 - 10 days PMI (0-90 ADD), evening  
417 surveys optimal for 10-40 days PMI (90-400 ADD) and midday/evening surveys  
418 optimal from 50 days PMI to the end of the 61 day PMI (680 ADD) survey period.

419 Study limitations included using one and not multiple pig cadavers for replication  
420 purposes, one naked deposition style and of course this was undertaken on one  
421 study site, with unique soil compositions and local vegetation type. Replicating the  
422 study using replicate pig cadavers in different depositional styles (i.e. wrapped in  
423 carpet/plastic sheeting, clothed) will undoubtedly have different thermal signatures  
424 and thus should be undertaken. Finally, this should be repeated using UAVs, or  
425 indeed helicopter-mounted thermal cameras as these are commonly used in Police  
426 active searches.

427

428 **References**

- 429 1. Pringle JK, Ruffell A, Jervis JR, Donnelly L, McKinley J, Hansen J, et al. The  
430 use of geoscience methods for terrestrial forensic searches. *Earth Sci Rev*  
431 2012;114:108–23.
- 432 2. Ruffell A, Pringle JK, Cassella JP, Morgan M, Ferguson M, Heaton VG, et al.  
433 The use of geoscience for aquatic forensic searches. *Earth Sci Rev*  
434 2017;171:323-37.
- 435 3. Kalacska M, Bell LS, Sanchez-Azofeifa GA, Caelli T. The application of  
436 remote sensing for detecting mass graves: an experimental animal case study  
437 from Costa Rica. *J Forensic Sci* 2009;54:159–66.
- 438 4. Harrison M, Donnelly LJ. Locating concealed homicide victims: developing the  
439 role of geoforensics. In: Ritz K, Dawson L, Miller D, editors. *Criminal and*  
440 *environmental soil forensics*. Dordrecht: Springer, 2009;197–219.
- 441 5. Ruffell A, McKinley J. Forensic geomorphology. *Geomorphology*  
442 2014;206:14–22.
- 443 6. Caccianiga M, Bottacin S, Cattaneo C. vegetation dynamics as a tool for  
444 detecting clandestine graves, *J. Forensic Sci* 2012;57:983-88.
- 445 7. Aquila I, Ausania F, Di Nunzio C, Serra A, Boca S, Capelli A, et al. The role of  
446 forensic botany in crime scene investigation: case report and review of  
447 literature. *J Forensic Sci* 2014;59:820–4.
- 448 8. Amendt J, Campobasso CP, Gaudry E, Reiter C, Le Blanc HN, Hall MJR.  
449 Best practice in forensic entomology: standards and guidelines. *Int J Legal*  
450 *Med* 2007;121:90–104

- 451 9. Lasseter A, Jacobi KP, Farley R, Hensel L. Cadaver dog and handler team  
452 capabilities in the recovery of buried human remains in the Southeastern  
453 United States. *J Forensic Sci* 2003;48:617–21.
- 454 10. Riezzo I, Neri M, Rendine M, Bellifemina A, Cantatore S, Fiore C, et al.  
455 Cadaver dogs: unscientific myth or reliable biological devices? *Forensic Sci*  
456 *Int* 2014;244:213–21.
- 457 11. Ruffell A, McKinley J. *Geoforensics*. Chichester: Wiley, 2008.
- 458 12. Edelman GJ, Hoveling RJM, Roos M, van Leeuwen TG, Aalders MCG.  
459 Infrared imaging of the crime scene: possibilities and pitfalls, *J Forensic Sci*  
460 2013;58:1156-62.
- 461 13. Yamauchi S, Hitosugi M, Kimura H, Tokudome S. A novel application of  
462 infrared imaging for the diagnosis of death by fire. *J Forensic Sci*  
463 2013;58:1022-25.
- 464 14. de la Ossa ÁF, Amigob JM, García-Ruiza C. Detection of residues from  
465 explosive manipulation by near infrared hyperspectral imaging: A promising  
466 forensic tool, *Forensic Sci Int* 2014;242:228-35.
- 467 15. Edelman GJ, Gaston E, van Leeuwen TG, Cullen PJ, Aalders MCG.  
468 Hyperspectral imaging for non-contact analysis of forensic traces, *Forensic*  
469 *Sci Int* 2012;223:28-39.
- 470 16. Edelman GJ, van Leeuwen TG, Aalders MCG. Hyperspectral imaging for the  
471 age estimation of blood stains at the crime scene, *Forensic Sci Int*  
472 2012;223:72-77.
- 473 17. Deans J, Gerhard J, Carter LJ. Analysis of a thermal imaging method for  
474 landmine detection using infrared heating of the sand surface, *Infrared Phys*  
475 *Tech* 2006;48:202–16.

- 476 18. Gurton KP, Felton M. Remote detection of buried land-mines and IEDs using  
477 LWIR polarimetric imaging, *Opt Express* 2012;20:22344–59.
- 478 19. Stowell C. Thermal imaging by law enforcement, *Proc SPIE* 2001;4360:192–  
479 202.
- 480 20. Koukiou G, Anastassopoulos V. Neural networks for identifying drunk persons  
481 using thermal infrared imagery, *Forensic Sci Int* 2015;252:69-76.
- 482 21. France DL, Griffin TJ, Swanburg JG, Lindemann JW, Davenport GC,  
483 Trammell V, et al. A multidisciplinary approach to the detection of clandestine  
484 graves. *J Forensic Sci* 1992;37:1445–58.
- 485 22. Schultz JJ, Collins ME, Falsetti AB. Sequential monitoring of burials  
486 containing large pig cadavers using ground-penetrating radar. *J Forensic Sci*  
487 2006;51:607–16.
- 488 23. Schultz JJ. Sequential monitoring of burials containing small pig cadavers  
489 using ground-penetrating radar. *J Forensic Sci* 2008;53:279–87.
- 490 24. Schultz JJ, Martin MM. Controlled GPR grave research: comparison of  
491 reflection profiles between 500 and 250 MHz antennae. *Forensic Sci Int*  
492 2011;209:64–9.
- 493 25. Pringle JK, Jervis J, Cassella JP, Cassidy NJ. Time-lapse geophysical  
494 investigations over a simulated urban clandestine grave. *J Forensic Sci*  
495 2008;53:1405–17.
- 496 26. Pringle JK, Holland C, Szkornik K, Harrison M. Establishing forensic search  
497 methodologies and geophysical surveying for the detection of clandestine  
498 graves in coastal beach environments. *Forensic Sci Int* 2012;219:e29–36
- 499 27. Pringle JK, Jervis JR, Hansen JD, Cassidy NJ, Jones GM, Cassella JP.  
500 Geophysical monitoring of simulated clandestine graves using electrical and

- 501 Ground Penetrating Radar methods: 0-3 years. *J Forensic Sci* 2012;57:1467-  
502 86.
- 503 28. Pringle JK, Jervis JR, Roberts D, Dick HC, Wisniewski KD, Cassidy NJ, et al.  
504 Geophysical monitoring of simulated clandestine graves using electrical and  
505 ground penetrating radar methods: 4-6 years. *J Forensic Sci* 2016;61:309–21.
- 506 29. Jervis JR, Pringle JK, Tuckwell G. Time-lapse resistivity surveys over  
507 simulated clandestine graves. *Forensic Sci Int* 2009;192:7–13
- 508 30. Ruffell A, Pringle JK, Forbes S. Search protocols for hidden forensic objects  
509 beneath floors and within walls. *Forensic Sci Int* 2014;237:137– 45.
- 510 31. Henssge C, Madea B. Estimation of the time since death in the early post-  
511 mortem period. *Forensic Sci Int* 2004;144:167–75.
- 512 32. Faber P, Garby L. Fat content affects heat capacity: a study in mice. *Acta*  
513 *Physiol Scand* 1995;153:185-87.
- 514 33. Bristow KL, Kuitenberg GJ, Goding CJ, Fitzgerald TS. A small multi-needle  
515 probe for measuring soil thermal properties, water content and electrical  
516 conductivity. *Comp Elect In Agri* 2001;31:265-80.
- 517 34. Campobasso CP, Di Vella G, Introna F. Factors affecting decomposition and  
518 Diptera colonization, *Forensic Sci Int* 2001;120:18-27.
- 519 35. Grassberger M, Frank C. Initial study of arthropod succession on pig carrion  
520 in a Central European urban habitat. *J Med Entomol* 2004;41:511-23.
- 521 36. Slone DH, Gruner SV. Thermal regulation in larval aggregations of carrion-  
522 feeding blow flies (Diptera: Calliphoridae). *J Med Entomol* 2007;44:516-23.
- 523 37. VanLaerhoven SL. Blind validation of post-mortem interval estimates using  
524 developmental rates of blow flies. *Forensic Sci Int* 2008;180:76-80.

- 525 38. Amendt J, Richards CS, Campobasso CP, Zehner R, Hall MJ. Forensic  
526 Entomology: Application and Limitations. *Forensic Sci Med Pat* 2011;7:379-  
527 92.
- 528 39. Cross P, Simmons T. The influence of penetrative trauma on the rate of  
529 decomposition. *J Forensic Sci* 2010;55:295-301.
- 530 40. Heaton VG, Moffatt C, Simmons T. Quantifying the Temperature of Maggot  
531 Masses and its Relationship to Decomposition. *J Forensic Sci* 2014;59:676-  
532 82.
- 533 41. Richards EN, Goff ML. Arthropod succession on exposed carrion in three  
534 contrasting tropical habitats on Hawaii Island, Hawaii. *J Med Entomol*  
535 1997;34:328-39.
- 536 42. Richards CS, Price BW, Villet MH. Thermal ecophysiology of seven carrion-  
537 feeding blowflies in Southern Africa. *Entomol Exp Appl* 2009;131:11-19.
- 538 43. Charabidze D, Bourel B, Gosset D. Larval-mass effect: Characterisation of  
539 heat emission by necrophagous blowflies (Diptera: Calliphoridae) larval  
540 aggregates. *Forensic Sci Int* 2011;211:61-66.
- 541 44. Rivers DB, Ciarlo T, Spelman M, Brogan R. Changes in development and  
542 heat shock protein expression in two species of flies (*Sarcophaga bullata*  
543 [Diptera: Sarcophagidae] and *Protophormia terraenovae* [Diptera:  
544 Calliphoridae]) reared in different sized maggot masses. *J Med Entomol*  
545 2010;47:677-89.
- 546 45. Charabidze D, Bourel B, Hedouin V, Gossett D. Repellent effect of some  
547 household products on fly attraction to cadavers, *Forensic Sci Int*  
548 2009;189:28-33.

- 549 46. Joy JE, Liette NL, Harrah HL. Carrion fly (Diptera: Calliphoridae) larval  
550 colonisation of sunlit and shaded pig carcasses in West Virginia, USA.  
551 Forensic Sci Int 2006;164:183-92.
- 552 47. Pringle JK, Cassella JP, Jervis JR, A. Williams, Cross P, Cassidy NJ.  
553 Soilwater conductivity analysis to date and locate clandestine graves of  
554 homicide victims. J. Forensic Sci 2015a;60:1052-60.
- 555 48. Carter DO, Tibbett M. Cadaver decomposition and soil: processes, in: M.  
556 Tibbett, D.O. Carter, eds. Soil analysis in forensic taphonomy: chemical and  
557 biological effects of buried human remains. CRC Press, 2009;29–52.
- 558 49. Stokes KL, Forbes SL, Tibbett M. Human versus animal: contrasting  
559 decomposition dynamics of mammalian analogues in experimental  
560 taphonomy. J Forensic Sci 2013;58:583-91.
- 561 50. Soerensen DD, Clausen S, Mercer JB, Pedersen LJ. Determining the  
562 emissivity of pig skin for accurate infrared thermography. Comp Elect in Agri  
563 2014;109:52–58.
- 564 51. Lloyd JM. Thermal imaging systems. Boston MA, Springer 1975;18-30.
- 565 52. NASA (n.d.). Thermography. [Online] Available at  
566 [https://kscddms.ksc.nasa.gov/Reliability/Documents/Preferred\\_Practices/at9.p](https://kscddms.ksc.nasa.gov/Reliability/Documents/Preferred_Practices/at9.pdf)  
567 [df](https://kscddms.ksc.nasa.gov/Reliability/Documents/Preferred_Practices/at9.pdf). [Accessed 02/10/2019]
- 568 53. Havens KJ, Sharp EJ, editors. Thermal imaging techniques to survey and  
569 monitor animals in the wild. Academic Press, 2016;89-99.
- 570 54. Steketee J. Spectral emissivity of skin and pericardium, Phys in Med & Bio  
571 1973;18:686-94.

- 572 55. Megyesi MS, Nawrocki SP, Haskell NH. Using accumulated degree-days to  
573 estimate the postmortem interval from decomposed human remains. J  
574 Forensic Sci 2005;50:618-26
- 575 56. Johnson A, Wallman J. Infrared imaging as a non-invasive tool for  
576 documenting maggot mass temperatures. Australian J Forensic Sci  
577 2014;46:73-78.
- 578 57. Amendt J, Rodner S, Schuch CP, Sprenger H, Weidlich L, Reckel F.  
579 Helicopter thermal imaging for detecting insect infested cadavers. Sci Justice  
580 2017;57:366–72.
- 581 58. DesMarais AM. Detection of Cadaveric Remains by Thermal Imaging  
582 Cameras. J Forensic Identif 2014;64:489-510.
- 583 59. Pringle JK, Jervis JR. Electrical resistivity survey to search for a recent  
584 clandestine burial of a homicide victim, UK. Forensic Sci Int 2010;202: e1–7.
- 585 60. Greenberg B, Kunich JC. Entomology and the Law: Flies as Forensic  
586 Indicators. Cambridge University Press, 2002.
- 587 61. Lee MJ, Voss SC, Franklin D, Dadour IR. Preliminary investigation of aircraft  
588 mounted thermal imaging to locate decomposing remains via the heat  
589 produced by larval aggregations. Forensic Sci Int 2018;289:175-85.
- 590 62. Towne E. Prairie vegetation and soil nutrient responses to ungulate  
591 carcasses. *Oecologia*. 2000;122:232–239. [DOI 0.1007/PL00008851](https://doi.org/10.1007/PL00008851)
- 592 63. Martinelli F, Scalenghe R, Davino S, Panno S, Scuderi G, Ruisi P, Villa P.  
593 Advanced methods of plant disease detection. A review. Agron. Sustain. Dev.  
594 2015;35:1–25. DOI 10.1007/s13593-014-0246-1
- 595